

for these crucial experiments are exhibited for the specific case of the peracetate of [4S]-rhynchosporoside (**19b**). Thus in plot A (Figure 1) (^1H decoupled ^{13}C NMR spectrum) the anomeric signals are located at δ 100.79, 100.66, and 100.50 for the β -bonded carbons and at δ 95.53 for the α -bonded carbon. Plot B (Figure 1) (2D ^1H - ^{13}C heteronuclear chemical shift correlated spectrum)¹⁵ correlates the chemical shifts of the anomeric carbons with the respective anomeric protons which assisted in their assignment. These experiments provided a convenient and unambiguous way of establishing the stereochemical configuration of the rhynchosporosides, their high purity and the specificity of the reported coupling reactions.

With these rhynchosporosides now readily available in pure form by synthesis, their isolation from nature, structural elucidation, and biological evaluation becomes feasible. Preliminary bioassays with the tri-, tetra-, and pentasaccharides, for example, indicated high destructive potency for the [3R]-, [4R]-, and [5R]-rhynchosporosides **15a**, **19a**, and **25a** which caused massive tip wilt and necrosis in young barley plants.^{16,17}

Acknowledgment. We express our many thanks to Professors G. A. Strobel and P. Auriol for helpful discussions and biological investigations. We are also indebted to Dr. Manfred Spraul of Bruker Analytische Messtechnik GMBH, West Germany, for assistance in obtaining the high-field NMR data and John Dykins of this department for his mass spectroscopic assistance. This work was financially supported by Merck Sharp & Dohme, the Camille and Henry Dreyfus Foundation, and the National Institutes of Health.

Supplementary Material Available: Spectral and analytical data and structures for compounds **15a**, **15b**, **19a**, **19b**, **25a**, and **25b** (3 pages). Ordering information is given on any current masthead page.

(14) Bock, K.; Thogersen, H. *Annu. Rep. NMR Spectrosc.* **1982**, *13*, 1.

(15) Wong, T. C.; Rutar, V.; Wang, J.-S.; Feather, M.; Kovac, P. *J. Org. Chem.* **1984**, *49*, 4358.

(16) We thank Professor G. A. Strobel and Dr. F. Sugawara, Department of Plant Pathology, Montana State University, MT 59717-0002, for these biological results.

(17) All new compounds exhibited satisfactory spectroscopic and analytical and/or exact mass data. Yields refer to spectroscopically and chromatographically homogeneous materials.

Adsorption and Decomposition of Formaldehyde on the Ru(001) Surface: The Spectroscopic Identification of $\eta^2\text{-H}_2\text{CO}$ and $\eta^5\text{-HCO}$

A. B. Anton, J. E. Parmeter, and W. H. Weinberg*

*Division of Chemistry and Chemical Engineering
California Institute of Technology
Pasadena, California 91125*

Received May 6, 1985

The interaction of formaldehyde with transition-metal surfaces is of obvious importance in view of the fact that species such as $\text{M-CH}_2\text{O}$ and M-CHO may play a key role in the catalytic hydrogenation of carbon monoxide.¹⁻³ Recently, several organometallic complexes have been identified in which both formaldehyde⁴⁻⁷ and the formyl group⁸ function as dihapto (η^2 -

Table I. Mode Assignments for $\eta^2\text{-H}_2\text{CO}$ ($\eta^2\text{-D}_2\text{CO}$) on Ru(001)

mode	$\eta^2\text{-H}_2\text{CO}$, cm^{-1}	$\eta^2\text{-D}_2\text{CO}$, cm^{-1}	frequency ratio ($\text{H}_2\text{CO}/\text{D}_2\text{CO}$)
$\nu(\text{CO})$	980	1020	0.96
$\nu_3, \nu_4(\text{CH}_2)$	2940	2225	1.32
$\delta(\text{CH}_2)$	1450	1190	1.22
$\omega(\text{CH}_2)$	1160	865	1.34
$\rho(\text{CH}_2)$	840	620	1.35

Table II. Mode Assignments for $\eta^2\text{-HCO}$ ($\eta^2\text{-DCO}$) on Ru(001) with Corresponding Assignments from the Model Compound HCOOCH_3 (DCOOCH_3) (See Ref 15)

mode	$\eta^2\text{-HCO}$, cm^{-1}	HCOOCH_3 , cm^{-1}	$\eta^2\text{-DCO}$, cm^{-1}	DCOOCH_3 , cm^{-1}
$\nu(\text{CH})$	2900	2943	<i>a</i>	2216
$\delta(\text{CH})$	1400	1371	980	1048
$\nu(\text{CO})$	1180	1207	1160	1213
$\pi(\text{CH})$	1065	1032	825	870
$\nu(\text{Ru-HCO})$	590		550	

^a Weak and not resolved from the tail of the strong feature due to adsorbed CO at 1990 cm^{-1} .

ligands. In this paper, we report the results of high-resolution electron energy loss (HREELS) measurements of formaldehyde adsorbed on the hexagonally close-packed Ru(001) surface that demonstrate the existence of both $\eta^2\text{-H}_2\text{CO}$ and $\eta^2\text{-HCO}$. This represents the first spectroscopic identification of either species on any metal surface.

The ultrahigh vacuum (UHV) system in which the experiments were performed has been described previously.⁹ HREELS was used to identify surface reaction products after adsorption at 80 K, subsequent annealing up to 600 K, and recoiling to 80 K to record the spectra. Gaseous H_2CO and D_2CO were produced by thermal dehydration and depolymerization of their parent polyoxymethylene glycols (paraformaldehyde) and were introduced into the UHV chamber through a leak valve. The H_2CO (D_2CO) produced by this method contains 3-5% H_2O (D_2O) impurity,¹⁰ and, consequently, spectra recorded after heating below 170 K are expected to show vibrational features attributable to small amounts of coadsorbed water.¹¹

Exposing the Ru(001) surface at 80 K to 7 langmuirs (1 langmuir = 10^{-6} torr s) or more of H_2CO or D_2CO results in the formation of molecular multilayers of formaldehyde, as evidenced by a comparison of the observed vibrational spectra to the IR spectrum of gaseous formaldehyde.¹² Annealing the surface to 140 K desorbs the multilayer, leaving adsorbed carbon monoxide ($\theta = 0.20$ CO molecules/Ru surface atom),¹³ hydrogen adatoms ($\theta = 0.40$),¹⁴ and another surface species ($\theta = 0.10$) which is stable to approximately 250 K. This new species is identified as η^2 -formaldehyde. The spectra for H_2CO and D_2CO are shown at the top of Figure 1, and mode assignments are given in Table I. The observed CO stretching frequency of approximately 1000 cm^{-1} is consistent with a reduction in bond order of the CO bond from double to single and is in good agreement with the CO stretching frequency of 1017 cm^{-1} for $\eta^5\text{-H}_2\text{CO}$ in the organometallic compound $(\text{PPh}_3)_2(\text{CO})_2\text{Os}(\eta^5\text{-H}_2\text{CO})$.⁴ The observed frequencies and deuteration shifts for the various CH_2 modes agree well with those observed for $\text{sp}^3\text{-CH}_2$ groups in various molecules.¹⁵

(8) Belmonte, P. A.; Cloke, F. G. N.; Schrock, R. R. *J. Am. Chem. Soc.* **1983**, *105*, 2643-2650.

(9) Thomas, G. E.; Weinberg, W. H. *Rev. Sci. Instrum.* **1979**, *50*, 497-501.

(10) Walker, J. F. "Formaldehyde"; Reinhold: New York, 1964; p 142.

(11) Thiel, F. A.; Hoffmann, F. M.; Weinberg, W. H. *J. Chem. Phys.* **1981**, *75*, 5556-5572.

(12) Herzberg, G. "Infrared and Raman Spectra"; D. Van Nostrand Co.: New York, 1945; p 300.

(13) Thomas, G. E.; Weinberg, W. H. *J. Chem. Phys.* **1979**, *70*, 954-961, 1437-1439. Weinberg, W. H. *Methods Exp. Phys.* **1985**, *22*, 23-125.

(14) Barteau, M. A.; Broughton, J. Q.; Menzel, D. *Surf. Sci.* **1983**, *133*, 443-452.

(15) Shimanouchi, T. "Tables of Vibrational Frequencies"; Consolidated Vol. I, NSRDS-NBS 39, Vol. II.

(1) Muetterties, E. L.; Stein, J. *Chem. Rev.* **1979**, *79*, 479-490.

(2) Eisenberg, R.; Hendricksen, D. E. *Adv. Catal.* **1979**, *28*, 79-172.

(3) Dombek, B. D. *Adv. Catal.* **1983**, *32*, 325-416.

(4) Brown, K. L.; Clark, G. R.; Headford, C. E. L.; Marsden, K.; Roper, W. R. *J. Am. Chem. Soc.* **1979**, *101*, 503-505.

(5) Gambarotta, S.; Floriani, C.; Chiese-Villa, A.; Guastini, C. *J. Am. Chem. Soc.* **1982**, *104*, 2019-2020.

(6) Buhro, W. E.; Patton, A. T.; Strouse, C. E.; Gladysz, J. A.; McCormick, F. B.; Etter, M. C. *J. Am. Chem. Soc.* **1983**, *105*, 1056-1058.

(7) Kropp, K.; Skibbe, V.; Erker, G.; Krüger, C. *J. Am. Chem. Soc.* **1983**, *105*, 3353-3354.

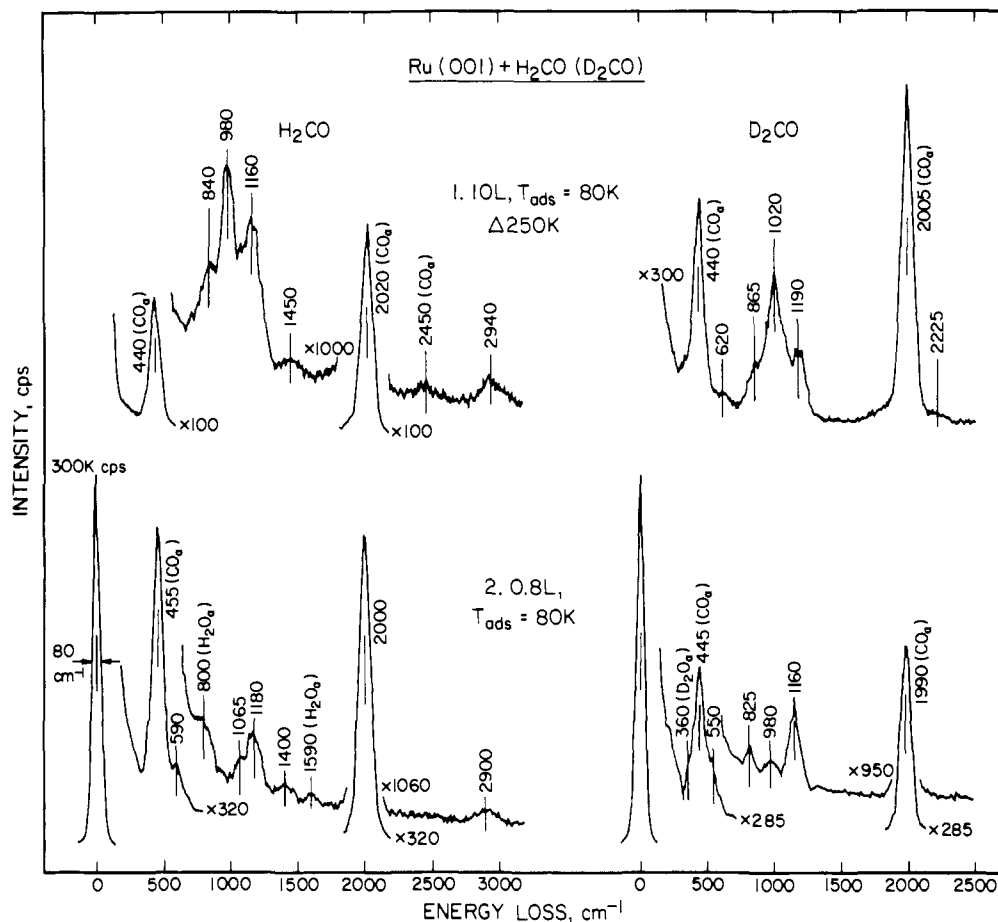


Figure 1. High-resolution electron energy loss spectra of (1) a multilayer exposure (10 langmuirs) of H_2CO (D_2CO) adsorbed on Ru(001) at 80 K and annealed to 250 K and (2) a submonolayer exposure (0.8 langmuir) of H_2CO (D_2CO) on Ru(001) at 80 K. The spectra in (1) are characteristic of η^2 -formaldehyde, and those in (2) are characteristic of η^2 -formyl. In all these spectra intense modes near 450 and 2000 cm^{-1} are due to adsorbed CO from formaldehyde decomposition, as is the weak combination band occasionally observed near 2450 cm^{-1} .¹³ Adsorbed hydrogen adatoms from formaldehyde decomposition are not observed due to their extremely small scattering cross section.¹⁴ Features at 800 and 1590 cm^{-1} in the H_2CO spectrum of (2) and near 360 cm^{-1} in the D_2CO spectrum of (2) are due to H_2O and D_2O ,¹¹ respectively, to which the crystal is exposed unavoidably during the adsorption of H_2CO and D_2CO at 80 K.

Spectra of lower coverages of H_2CO or D_2CO on Ru(001) at 80 K reveal a species that is fundamentally different from the η^2 -formaldehyde that results after annealing the formaldehyde multilayer. The spectra obtained after clean Ru(001) is exposed to 0.8 langmuir of H_2CO (or D_2CO) at 80 K are shown at the bottom of Figure 1. Although there is significant decomposition to adsorbed carbon monoxide ($\theta = 0.15$) and hydrogen ($\theta = 0.30$), additional loss features due to another adsorbed species ($\theta = 0.05$) are observed at 2900, 1400, 1180, 1065, and 590 cm^{-1} for H_2CO , and at 1160, 980, 825, and near 550 cm^{-1} for D_2CO . Heating to 100 K causes these features to disappear as this species decomposes to carbon monoxide adatoms and hydrogen adatoms. Weak features at 800 and 1590 cm^{-1} in the H_2CO spectrum and at 360 and 1150 cm^{-1} (obscured by the stronger mode at 1160 cm^{-1} associated with D_2CO adsorption in the spectrum of Figure 1) in the D_2CO spectrum persist to 170 K, the desorption temperature of water from the Ru(001) surface, and can be identified readily with librational and scissoring modes of small amounts of coadsorbed H_2O and D_2O , respectively.¹¹ The spectra in the bottom panel of Figure 1 can be identified unambiguously as an η^2 -HCO (η^2 -DCO) adspecies,⁸ and the mode assignments are given in Table II. The presence of the η^2 -formyl is perhaps not surprising in view of the fact that there is substantial decomposition of the formaldehyde to adsorbed carbon monoxide and hydrogen at low surface coverages, and η^2 -formaldehyde exists at saturation monolayer coverage. The formyl ligand, although not heretofore identified on a surface, has been observed as a product of the interaction of formaldehyde with metal centers in organometallic compounds.^{1,4,5} As would be expected, there is excellent agreement between the vibrational frequencies of the η^2 -HCO (η^2 -DCO)

bonded to the Ru(001) surface and the corresponding vibrational frequencies of the HCO (DCO) function of the "model compound" HCOOCH_3 (DCOOCH_3),¹⁵ of which the latter are listed in Table II. The mode at 590 cm^{-1} (550 cm^{-1}) for η^2 -HCO (η^2 -DCO) is assigned to the frustrated translation of the formyl perpendicular to the surface, its rather high frequency a natural consequence of the relatively low mass of HCO (DCO) and the stiffness of the (one) Ru-O and (two) Ru-C bonds which coordinate it to the surface.

The conditions that lead to the formation of η^2 -HCO and η^2 - H_2CO provide a consistent picture of the mechanism of H_2CO decomposition on the Ru(001) surface. The η^2 -HCO is favored over η^2 - H_2CO at low surface coverages because there exist vacant sites at which a hydrogen atom from the decomposing η^2 - H_2CO may bind. At higher coverages the absence of such vacant sites inhibits decomposition and favors the formation of η^2 - H_2CO . Indeed, precoverage of the Ru(001) surface by a saturation exposure (3 langmuirs) of H_2 , followed by exposure to H_2CO at 80 K, results in the formation of η^2 - H_2CO at all submonolayer coverages, with essentially no dissociation to adsorbed CO and hydrogen at 80 K.

The spectroscopic identifications put forward in this paper have been confirmed by off-specular HREELS measurements, thermal desorption mass spectrometry results, and complementary experiments concerning H_2CO and D_2CO adsorption on the Ru(001) surface modified by the presence of a $p(2 \times 2)$ ordered overlayer of oxygen adatoms. A complete discussion of all of these results will be presented separately.¹⁶

(16) Anton, A. B.; Parmeter, J. E.; Weinberg, W. H., unpublished results.

Acknowledgment. This research was supported by the National Science Foundation under Grant CHE-8206487. The assistance of Dr. Neil Avery in the early stages of this work is very much appreciated.

Ab Initio Mechanisms for the Addition of CH_3Li , HLi , and Their Dimers to Formaldehyde

Elmar Kaufmann and Paul von Ragué Schleyer*

Institut für Organische Chemie der
Friedrich-Alexander-
Universität Erlangen-Nürnberg
D-8520 Erlangen, Federal Republic of Germany

K. N. Houk* and Yun-Dong Wu

Department of Chemistry, University of Pittsburgh
Pittsburgh, Pennsylvania 15260

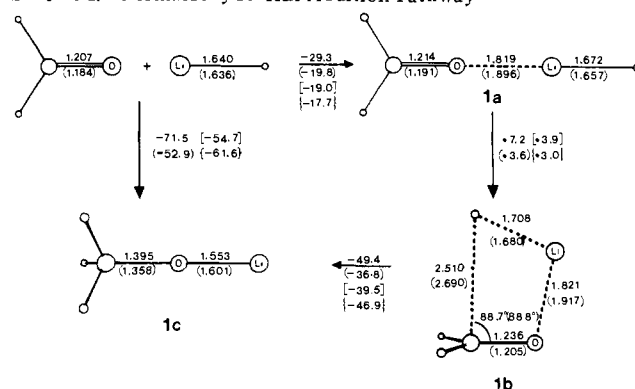
Received August 8, 1984

Although the reactions of alkyllithiums with carbonyl compounds are among the most elementary synthetic reactions,¹ little detailed mechanistic information is available. By use of rapid injection NMR, McGarrity et al. have shown that butyllithium dimer in tetrahydrofuran reacts about 10 times faster than the tetramer with benzaldehyde.^{2,3} Even at high dilution, there is no detectable concentration of monomer. Hence, contrary to earlier suggestions based on kinetic evidence,⁴ the monomer does not appear to be the reactive intermediate in ether solvents.

We now report an ab initio examination⁵ of the mechanisms of model reactions of formaldehyde with the monomers CH_3Li and LiH , as well as with their dimers. The performance of the split valence 3-21G basis set, used for all these systems, was evaluated at higher levels for the $\text{HLi} + \text{H}_2\text{CO}$ process (see caption, Scheme I) and should be reasonably reliable for the larger systems (Schemes II-IV).

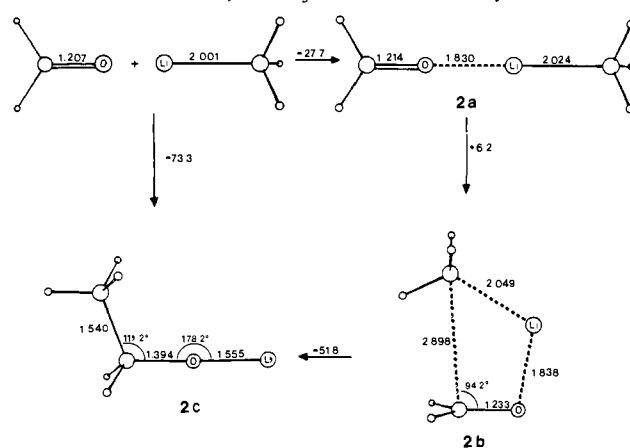
All four reaction pathways (Schemes I-IV) are rather similar; each proceeds in three stages. Formaldehyde complexes with the lithium reagents **1a-4a** are formed first.^{4,6} Since the association

Scheme I. Formaldehyde-HLi Addition Pathway^a

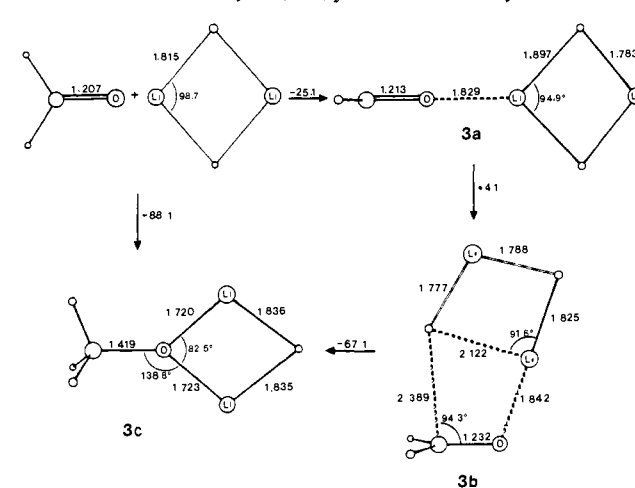


^a Energies in kcal/mol, distances in Å, angles in deg. Data at 3-21G//3-21G are compared with optimized (6-31G**//6-31G*) as well as with single point [6-31+G**//6-31G*] and {MP2/6-31+G**//6-31G*} values.

Scheme II. Formaldehyde- CH_3Li Addition Pathway



Scheme III. Formaldehyde-(HLi)₂ Addition Pathway



is quite exothermic,⁷ the bonds in the complexes are lengthened slightly. Complexes **1a-4a** next convert to the addition transition structures ("states" is less satisfactory nomenclature) **1b-4b**; each is characterized by having a single imaginary frequency. In all four cases, the activation energies are quite small. The last stage of each reaction, conversion to ROLi (**1c** or **2c**) or to a ROLi-RLi mixed dimer (**3c** or **4c**), is very exothermic, as is the overall energy.

(7) See Del Bene, J. E.; Frisch, M. J.; Raghavachari, K.; Pople, J. A.; Schleyer, P. v. R. *J. Phys. Chem.* **1983**, *87*, 73 and references cited. Kaufmann, E., unpublished calculations. Smith, S. F.; Chandrasekhar, J.; Jorgensen, W. L. *J. Phys. Chem.* **1982**, *86*, 3308.

(1) Wakefield, B. J. "The Chemistry of Organolithium Compounds"; Pergamon Press: Oxford, 1974. Eicher, T. In "The Chemistry of the Carbonyl Group"; Patai, S., Ed.; Interscience Publishers: London, 1966.

(2) McGarrity, J. F.; Ogle, C. A.; Brich, Z.; Loosli, H.-R. *J. Am. Chem. Soc.* **1985**, *107*, 1810. Also see: McGarrity, J. F.; Ogle, C. A. *Ibid.* **1985**, *107*, 1805. See: Bacn, D.; Hassig, R.; Gabriel, J. *Helv. Chim. Acta* **1983**, *66*, 308.

(3) McGarrity, J. F.; Prodollet, J.; Smyth, T. *Org. Magn. Reson.* **1981**, *17*, 59. McGarrity, J. F.; Prodollet, J. *J. Org. Chem.* **1984**, *49*, 4465.

(4) (a) Smith, S. G.; Charbonneau, L. F.; Novak, D. P.; Brown, T. L. *J. Am. Chem. Soc.* **1972**, *94*, 7059. In hydrocarbon solvents: (b) Charbonneau, L. F.; Smith, S. G. *J. Org. Chem.* **1976**, *41*, 808. Al-Aseer, M. A.; Smith, S. G., *J. Org. Chem.* **1984**, *49*, 2608. Al-Aseer, M. A.; Allison, B. D.; Smith, S. G. *Ibid.* **1985**, *50*, 2715. For criticisms of the interpretation of such kinetic results, see: References 1 (p 14), 2, and: (c) Brown, T. L. *J. Organomet. Chem.* **1966**, *5*, 191; *Adv. Organomet. Chem.* **1965**, *3*, 365.

(5) All calculations used the GAUSSIAN82 program: Binkley, J. S.; Frisch, M.; Raghavachari, K.; DeFrees, D.; Schlegel, H. B.; Whiteside, R.; Fluder, E.; Seeger, R.; Pople, J. A. Carnegie-Mellon University (adapted to CYBER 845 computer by Sawaryn, A.). All geometries were fully optimized and the transition structures characterized by frequency analysis. 3-21G optimized energies (au): **1a**, -121.198 41; **1b**, -121.186 95; **1c**, -121.265 67; **2a**, -160.018 56; **2b**, -160.008 59; **2c**, -160.091 19; **3a**, -129.195 13; **3b**, -129.188 60; **3c**, -129.295 52; $(\text{CH}_3\text{Li})_2$, -93.578 67; **4a**, -206.838 53; **4b**, -206.823 60; **4c**, -206.942 65; the other energies are taken from: "Carnegie-Mellon Quantum Chemistry Archive"; 3rd ed.; Whiteside, R. A., Frisch, M. J., Pople, J. A., Eds.; Carnegie-Mellon University, 1983. The absolute energies at 6-31G**//6-31G*, 6-31+G**//6-31G*, and MP2/6-31+G**//6-31G*, respectively: **1a**, -121.878 72, -121.882 48, -122.198 69; **1b**, -121.872 95, -121.876 26, -122.193 94; **1c**, -121.931 55, -121.939 25, -122.268 63; LiH , -7.980 87, -7.981 01, -7.996 15; H_2CO , -113.866 33, -113.871 14, -114.174 27.

(6) (a) For spectroscopic evidence for RLi -ketone complexes, see: Lozach, D.; Mollé, G.; Bauer, P.; Dubois, J. E. *Tetrahedron Lett.* **1983**, *24*, 4213. (b) The X-ray structure of $(\text{LiBr})_2$ solvated by four acetone molecules is reported in: Amstutz, R. Dissertation, ETH Zürich, 1983. For other, related examples see: a review: Setzer, W.; Schleyer, P. v. R. *Adv. Organomet. Chem.* **1985**, *24*, 353.